The E3 ligase TRIM31 regulates hematopoietic stem cell homeostasis and MLL-AF9 leukemia

Kai Zhang,[1,*] Dingdong Liu,[1,*] Yafei Li,[1] Zhencan Shi,[2] Jun Guo,[2] Chengjiang Gao,[3] Hu Wang,[1] Zhenyu Ju[1] and Daojun Diao[1]

[1]Key Laboratory of Regenerative Medicine of Ministry of Education, Institute of Aging and Regenerative Medicine, Jinan University, Guangzhou; [2]Department of Cardiology, the First Affiliated Hospital of Jinan University, Guangzhou and [3]Department of Immunology and Key Laboratory of Infection, Immunity of Shandong Province, Shandong University School of Basic Medical Sciences, Jinan, China.

**KZ and DL contributed equally as first authors.*

Correspondence: D. Diao
diaodaojun@hotmail.com

Z. Ju
zhenyuju@163.com

Received: August 18, 2022.
Accepted: December 28, 2022.
Early view: January 12, 2023.

https://doi.org/10.3324/haematol.2022.281955

©2023 Ferrata Storti Foundation
Published under a CC BY-NC license

Supplementary information

Supplemental methods

Transplantation assay

For HSC transplantation, 4000 LSK cells or 300/400 LT-HSCs ($CD48^-CD150^+$) were sorted via FACS, mixed with 1×10^6 or $3 \times 10^5/4 \times 10^5$ competitor BM cells respectively and transplanted into lethally irradiated mice. For the second transplantation, $1x10^6$ BM cells from the first transplantation mice were injected into the second-round recipient mice.

Cell cycle analysis

Cell cycle analysis was performed via BrdU and Ki67 staining. BrdU incorporation assay was utilized to determine the proliferation rate of HSCs. For *in vivo* analysis, BrdU (100 mg/kg; BD Biosciences) was injected i.p. into WT or *TRIM31*$^{-/-}$ mice once followed by administration of BrdU (1 mg/ml in water) for 10 days. BrdU incorporation and Ki67 staining was determined by FACS analysis using a BrdU and Ki67 Flow Kit (BD Biosciences) according to the manufacturer's instructions.

Ubiquitination assay

For analysis of the ubiquitination of CDK8 and CDK6 in hematopoietic cells, 1×10^7 enriched Lin^- cells from WT and *TRIM31*$^{-/-}$ mice were placed in SFEM and cultured after 30 min. The cells were treated with the proteasome inhibitor MG132 (20 μM, Calbiochem) for 5 h. The whole-cell extracts were immuno-precipitated with the specific antibody and analyzed by immunoblotting with an anti-Ub antibody (Santa Cruz Biotechnology).

Coimmunoprecipitation and mass spectrometry (MS) analysis

According to a previous immunoprecipitation method, enriched Lin^- cells from WT and *TRIM31*$^{-/-}$ mouse bone marrow were used. Co-IP was performed using an anti-TRIM31 antibody, and the IP product of WT cells was sent to the company (Shanghai Applied Protein Technology Co. Ltd) for mass spectrometry analysis. Samples from *TRIM31*$^{-/-}$ cells served as the control group. In the coomassie gel of WT and *TRIM31*$^{-/-}$ cells, the specific areas were cutted for the MS analysis (see figure legend). Briefly, the mass spectrometry analysis was performed as follows: Pieces were cut from SDS-PAGE gels, and LC-MS/MS analysis was performed on a Q Exactive mass spectrometer (Thermo Scientific), which was coupled to an Easy nLC instrument (Proxeon Biosystems, now Thermo Fisher Scientific) for protein identification. MS/MS spectra were searched using the MASCOT engine (Matrix Science, London, UK; version 2.2) against the UniProt Mus musculus database v3.85.

Coimmunoprecipitation and immunoblot analysis

For immunoblot analysis, cells were lysed with RIPA buffer supplemented with a protease inhibitor 'cocktail'. Protein concentrations in the extracts were measured with a bicinchoninic acid (BCA) assay (Pierce) and samples were made equal in amount and volume with extraction reagent. For immunoprecipitation (IP), the cells were lysed in IP buffer containing 1.0% (vol/vol) NP-40, 50 mM Tris-HCl (pH 7.4), 50 mM EDTA, 150 mM NaCl, and a protease inhibitor cocktail (Merck, Darmstadt, Germany). After centrifugation for 10 min at 14,000 g, supernatants were collected and incubated with protein G Plus Agarose Immunoprecipitation reagent (Santa Cruz Biotechnology) and 1-2 μg of the corresponding antibodies. After 6 h of incubation, the beads were washed five times with IP buffer. Immunoprecipitates were eluted by boiling with 1% (wt/vol) SDS sample buffer (60 mM Tris-HCl (pH 6.8), 1% (wt/vol) SDS, 5% (vol/vol) glycerol, 0.005% (wt/vol) bromophenol blue and 1% (vol/vol) 2-mercaptoethanol). For immunoblot analysis, immunoprecipitates or whole-cell

lysates were loaded and subjected to SDS-PAGE, transferred onto nitrocellulose membranes and then blotted with specific antibodies.

5-FU administration

5-FU (150 mg/kg) was injected into mice. The mice were sacrificed at the indicated time points and analyzed via fluorescence-activated cell sorting (FACS). Two times 5-FU injection were performed at 7 days interval, and most of the mice died within 30 days. Survival curves were generated according to the time of death of the mice.

Single-cell colony formation assay

Single cells were cultured for 14 days in 96-well plates containing liquid medium (SFEM medium) supplemented with 10% fetal bovine serum (FBS, Life Technologies), 20% BIT 9500 (Stem Cell Technologies), 5×10^{-5} M β-ME (Sigma-Aldrich), 10 ng/ml stem cell factor (SCF, Pepro Tech), 10 ng/ml thrombopoietin (TPO, Pepro Tech), 10 ng/ml Interleukin-3 (IL-3, Pepro Tech), 2 mM L-glutamine (Life Technologies) and 100 U/ml penicillin/streptomycin. The colonies were defined into three classes: large colonies consisting of more than 10,000 cells, intermediate colonies consisting of more than 1000 cells and small colonies consisting of more than 100 cells.

Intracellular staining of CDK8, EIF5A and Cdkn2a

BM cells (1×10^{7}) were stained with combinations of antibodies against cell-surface markers as described. After being washed with staining buffer, the cells were fixed in Cytofix/Cytoperm Fixation and Permeabilization Solution (BD) for 30 min. Fixed cells were stained with anti-CDK8, anti-EIF5A and anti-Cdkn2a antibodies in permeabilization solution for 30 min. The cells were washed and stained with

secondary antibodies before analyzing by using a Fortessa flow cytometer (BD).

Stem cell culture

For stem cell culture, cells were cultured in serum-free expansion medium (SFEM) (Stem Cell Technologies) supplemented with SCF (stem cell factor, 50 ng/mL, Pepro Tech), TPO (thrombopoietin, 50 ng/mL, Pepro Tech), and 100 U/mL penicillin/streptomycin.

Immunofluorescence analysis

Hematopoietic stem cells were sorted, placed on 0.01% poly l-lysine-treated cover slips and fixed with 4% PFA for 30 min at room temperature, followed by permeabilization with 0.5% Triton X-100 for 20 min at room temperature. Goat serum (10%) was used for blocking, and primary antibodies (in a 1:100 dilution) were added and incubated with the cells at room temperature for 2 h. After washing with PBS, the cover slips were stained with Alexa Fluor 488- and 594-conjugated secondary antibodies. Images were obtained with laser scanning confocal microscopy (Olympus FV500).

Quantitative reverse transcriptase-polymerase chain reaction

Total RNA was isolated using an RNeasy Micro Kit (Qiagen) and reverse transcribed using PrimeScript RT Master Mix (TaKaRa Biotechnology). Real-time PCR for the genes was performed using KAPA SYBR FAST qPCRKits (Kapa Biosystems) on a CFX 96 Real-time System (Bio-Rad). The amount of target RNA was normalized to that of the endogenous control β-actin. The gene expression quantities were determined according to the relative Ct method. The primers used in the experiments are summarized in Supplementary Tables 2 and 3.

Treatment of mice with CDK8 inhibitor

WT and *TRIM31*$^{-/-}$ mice were injected with the CDK8 inhibitor LY2857785 (intraperitoneal injection) at a dose of 7.5 mg/kg every other day for 14 days. The mice were sacrificed, bone marrow was analyzed via FACS, and the LT-HSCs were sorted for mouse transplantation.

Lentivirus production

shRNA lentivirus was produced in 293T cells after transfection with 15 mg SF-LV-shRNA-EGFP plasmid, 10 mg PSPAX2 helper plasmid and 6 mg pMD2G according to standard procedures. Gene overexpression Lentivirus was produced in 293T cells after transfection with 15 mg pLV-C-GFPSpark (Sino Biological) plasmid, 10 mg PSPAX2 helper plasmid and 6 mg pMD.G according to standard procedures. Virus was concentrated by centrifugation at 25,000 rpm for 2.5 h, 4 °C, and the virus pellet was resuspended in sterile PBS.

Lentivirus-mediated shRNA knockdown and gene overexpression

For gene knockdown and overexpression, 800 sorted LT-HSCs (CD48-CD150+ LSK) were cultured in serum-free expansion medium (SFEM) (Stem Cell Technologies) supplemented with 50 ng/mL stem cell factor (Pepro Tech), 50 ng/mL thrombopoietin (Pepro Tech), and 100 U/mL penicillin/streptomycin. The LT-HSCs were transduced with an appropriate amount of shRNA or overexpression lentivirus for 12 hrs. After twelve hours of culture, half of the LT-HSCs were mixed with 5×10^5 CD45.1 BM cells and then injected into recipient mice subjected to 8Gy x-ray irradiation. The left half of LT-HSCs was cultured further in SFEM for 60h and analyzed via fluorescence-activated cell sorting (FACS) to obtain the percentage of GFP-positive

cells at the zero time point. The shRNA sequences used in the knockdown experiments are listed in Supplementary Table 3.

Quantitative fluorescence in situ hybridization

Leukemia cells were deposited on charged slides by Cytospin (Thermo Fisher Scientific, USA), then fixed, permeabilized and stained with MLL (green) - AF9 (red) probes (Jinlu Bio, China). Slides were viewed under a Zeiss Laser scanning confocal microscope, LSM880 (Zeiss, Germany). Images were captured using ZEN lite software (Zeiss, Germany). At least five areas (100 cells) per sample were counted.

Quantification and Statistical Analysis

Data are presented as the mean ± standard deviation and were analyzed using GraphPad Prism 6. The statistical significance of differences between groups was calculated using an unpaired Student's t test. The survival curve was analyzed using a log-rank (Mantel-Cox) test.

Figure S1. *TRIM31* deletion impairs maintenance of progenitors.

(A) The relative mRNA expression of *TRIM31* was detected at 0 h, 24 h, and 48 h after the stimulation of HSC proliferation and differentiation with addition of cytokines (TPO, SCF and IL3), and the relative expression was normalized to beta-actin expression for statistical analysis (n = 3 per group). (B) Sanger sequencing after PCR was performed on the DNA from WT， TRIM31$^{+/-}$ and TRIM31$^{-/-}$ mouse. (C) Immunoblot of TRIM31 in Lin^{-} cell lysates from WT and TRIM31$^{-/-}$ mice. Beta-actin was used as a loading control (n = 3 per group). (D-F) The absolute number of bone marrow and Lin- cells in WT and *TRIM31*$^{-/-}$ mice (n = 5-6 per group) is indicated. Representative fluorescence-activated cell sorting (FACS) plots of the Lin- population are shown. (G) Representative FACS plots of the LK (Lin^{-}c-Kit^{+}Sca-1^{-}, LKS^{-}) and CLP (common lymphoid progenitor) populations are indicated. (H) The absolute number of LK (Lin^{-}c-Kit^{+}Sca-1^{-}, LKS^{-}) cells in WT and *TRIM31*$^{-/-}$ mice is shown (n = 5-6 per group). (I) The absolute number of CLPs in WT and *TRIM31*$^{-/-}$ mice is indicated (n = 5-6 per group). (J) Representative FACS plots of the Lin- and GMP populations in c-Kit positive cells of WT and *TRIM31*$^{-/-}$ mice are indicated. (K) The percentage in GMP in c-Kit positive cells of WT and *TRIM31*$^{-/-}$ mice are indicated (n = 4-5 per group). All results are presented as the means ± SD. *p<0.05; **p<0.01; ***p<0.001; NS=not significant. Notes: Eight- to twelve-week-old WT and *TRIM31*$^{-/-}$ mice were used in the experiments.

Figure S2. B cells and erythrocytes were affected in *TRIM31*$^{-/-}$ bone marrow.

(A) Representative FACS plots of B (B220^{+}) cells in WT and *TRIM31*$^{-/-}$ mice are shown. (B) The absolute numbers of T (CD4/8^{+}) cells, B cells, and myeloid (CD11b^{+}) cells in bone marrow from WT and *TRIM31*$^{-/-}$ mice are shown (n = 5-6 per group). (C) The composition of T cells, B cells and myeloid cells in PB from WT and *TRIM31*$^{-/-}$ mice is indicated (n = 3-6 per group). (D,E) FACS plots of the erythrocyte development stages are shown, which inculde E2 (TER119^{+}CD71^{hi}), E3

(TER119^{+}CD71^{mi}) and E4 (TER119^{+}CD71^{lo}) cells. The percentage in total of E2, E3 and E4 cells in WT and *TRIM31*$^{-/-}$ mice are indicated (n = 5-6 per group). All results are presented as the means ± SD. *p<0.05; **p<0.01; ***p<0.001; NS=not significant. Notes: Eight- to twelve-week-old WT and *TRIM31*$^{-/-}$ mice were used in the experiments.

Figure S3. *TRIM31* deficiency causes mouse spleen abnormalities.

(A,B) Representative spleen images and the relative weights of spleens in WT and *TRIM31*$^{-/-}$ mice are shown (n = 5 per group). (C,D) The percentages of LSK (Lin^{-}Sca-1^{+}c-Kit^{+}) cells, T cells, B cells and myeloid cells in spleens from WT and *TRIM31*$^{-/-}$ mice are indicated (n = 3-6 per group). (E) Experimental schematic illustrating serial competitive transplantation with WT or *TRIM31*$^{-/-}$ LT-HSCs. All results are presented as the means ± SD. *p<0.05; **p<0.01; ***p<0.001; NS=not significant. Notes: Eight- to twelve-week-old WT and *TRIM31*$^{-/-}$ mice were used in the experiments.

Figure S4. *TRIM31* deletion impairs the self-renewal capacity of LSK cells.

(A) Experimental schematic showing competitive transplantation with WT or *TRIM31*$^{-/-}$ LSK cells (results in B-E). (B) The percentage of donor-derived PB cells at the indicated time points in the LSK competitive transplantation assay is shown (n = 5 per group). (C) Percentage of donor-derived LSK (Lin^{-}Sca-1^{+}c-Kit^{+}) cells 24 weeks after competitive transplantation (n = 5 per group). (D) Percentage of donor-derived LT-HSCs (CD34^{-}Flt3^{-} LSK), ST-HSCs (CD34^{+}Flt3^{-} LSK) and MPP (CD34^{+}Flt3^{+} LSK) cells 24 weeks after competitive transplantation is shown (n = 5 per group). (E) Percentage of donor-derived LT-HSCs (CD48^{-}CD150^{+}Flt3^{-} LSK), ST-HSCs (CD48^{-}CD150^{-}Flt3^{-} LSK) and MPP (CD48^{+}Flt3^{-} LSK) cells 24 weeks after competitive transplantation is shown (n = 5 per group). (F-H) 4000 purified LSK cells

was transplanted along with $1x10^6$ fresh competitors each time. Chimerism of T, B and Myeloid cells in PB is shown at the indicated time points after transplantation. (I) Experimental schematic illustrating competitive transplantation with WT LSKs. (J) 4000 wild-type LSK cells was transplanted into wild-type and *TRIM31*$^{-/-}$-recipient mice. Percentage of donor-derived LSK ($Lin^-Sca\text{-}1^+c\text{-}Kit^+$) cells 12 weeks after competitive transplantation (n = 5 per group). All results are presented as the means ± SD. *p<0.05; **p<0.01; ***p<0.001; NS=not significant. Notes: Eight- to twelve-week-old WT and *TRIM31*$^{-/-}$ mice were used in the experiments.

Figure S5. *TRIM31* deletion leads to enhanced HSC proliferation.

(A) Representative FACS plots showing the Ki67 analysis in LT-HSCs ($CD48^-CD150^+Flt3^-$ LSK) and LSK cells. The percentage of G0,G1,S/G2/M phase cells is shown. (B-D) The percentage of G0,G1,S/G2/M phase cells among LT-HSCs and LSK cells from WT and *TRIM31*$^{-/-}$ mice (n = 5-6 per group). (E) Kaplan–Meier survival curve analysis of GSE 6891 dataset comparing the high (n =5) versus low (n = 5) of AML patients with 11q23 translocation based on *TRIM31* expression. (F) Log2-transformed expression of TRIM31 from microarray-based gene expression profiling of human AML patients cells (Bloodspot). All results are presented as the means ± SD. *p<0.05; **p<0.01; ***p<0.001; NS=not significant. Notes: Eight- to twelve-week-old WT and *TRIM31*$^{-/-}$ mice were used in the experiments.

Figure S6. *TRIM31* deficiency accelerated leukemia initiation.

(A) Schematic representation of the experiment. c-Kit^+ cells were enriched from the bone marrow of WT or *TRIM31*$^{-/-}$ mice, and transduced in vitro with retrovirus encoding MLL-AF9. After 72 hours, GFP-positive cells were sorted by FACS Aria 3 and $5x10^4$ GFP^+ was transplanted together with $5x10^5$ bone marrow cells into lethally irradiated recipients. (B) Representative pictures of colonies of

GFP-MLL-AF9–transformed WT or *TRIM31*$^{-/-}$ cells after 10 days in culture. (C) Colony number of GFP-MLL-AF9–transformed WT or *TRIM31*$^{-/-}$ cells after 10 days in First plating. (D) Colony number and cell number of GFP-MLL-AF9–transformed WT or *TRIM31*$^{-/-}$ cells after 10 days in second plating. (E) The mRNA level of MLL-AF9 in GFP+ cells from recipient mice transplanted with MLL-AF9 WT and *TRIM31*$^{-/-}$ cells was measured via real-time PCR. The relative expression was normalized to β-actin expression for statistical analysis (n = 3 per group). (F) Quantitative fluorescence in situ hybridization analysis showing the integrations and copies of MLL-AF9 fusion gene in leukemia cells from recipient mice transplanted with MLL-AF9 WT and *TRIM31*$^{-/-}$ donors. (G) The copy numbers of MLL (green) -AF9 (red) fusion gene in leukemia cells from recipient mice transplanted with MLL-AF9 WT and *TRIM31*$^{-/-}$ donors (n = 3 per group). (H, I) The MFI of GFP in GFP+ cells 48h and 72h after MLL-AF9 virus infected (n = 3 per group). (J) The MFI of GFP in GFP+ cells from recipient mice transplanted with MLL-AF9 WT and *TRIM31*$^{-/-}$ cells. All results are presented as the means ± SD. *p<0.05; **p<0.01; ***p<0.001; NS=not significant. Notes: Eight- to twelve-week-old WT and *TRIM31*$^{-/-}$ mice were used in the experiments.

Figure S7. CDK8 associates with Cyclin D1 in hematopoietic cells.

(A) The schematic diagram of coomassie gel was shown, anti-TRIM31 was performed in the whole cell lysate of WT and *TRIM31*$^{-/-}$ Lin^{-} cells, lanes in the red frame were cut and sent for MS analysis. (B) The MFI of EIF5A in LT-HSCs (CD48^{-}CD150^{+}Flt3^{-} LSK), LSK (Lin^{-}Sca-1^{+}c-Kit^{+}) cells and Lin^{-} cells from WT and TRIM31$^{-/-}$ mice is shown (n = 5 per group). (C) The MFI of Cdkn2a in LT-HSCs (CD48^{-}CD150^{+}Flt3^{-} LSK), LSK (Lin^{-}Sca-1^{+}c-Kit^{+}) cells and Lin^{-} cells from WT and TRIM31$^{-/-}$ mice is shown (n = 3 per group). (D) Immunoblot of CDK6 in WT and *TRIM31*$^{-/-}$ cell lysates. Beta-actin was used as a loading control (n = 3 per group). (E) Ubiquitination assay of CDK6 in the whole cell lysate from WT and *TRIM31*$^{-/-}$ mice. Immunoblot (IB) against

ubiquitin (Ub) was performed for the IP assay precipitate of CDK6 and CDK6 from whole lysate was used as a loading control. (F) Representative colocalization images of CDK8 (red) and Cyclin D1 (green) in HSCs are shown. All results are presented as the means ± SD. *p<0.05; **p<0.01; ***p<0.001; NS=not significant. Notes: Eight- to twelve-week-old WT and *TRIM31*$^{-/-}$ mice were used in the experiments.

Figure S8. Inhibition and knockdown of CDK8 rescues *TRIM31*$^{-/-}$ HSC function

(A) Experimental schematic showing CDK8 inhibitor (LY2857785) mouse treatment and subsequent competitive transplantation with LT-HSCs (results in B-D). Wild-type and *TRIM31*$^{-/-}$ mice were administered a CDK8 inhibitor (LY2857785) for 2 weeks, and 400 LT-HSCs were sorted and transplanted into recipient mice with $4x10^5$ competitors. (B) Percentage of donor-derived PB cells 8 weeks after competitive transplantation in LT-HSCs sorted from WT and TRIM31$^{-/-}$ mice treated with a CDK8 inhibitor (LY2857785) (n = 4 per group). (C, D) Percentage of donor-derived LSK ($Lin^-Sca\text{-}1^+c\text{-}Kit^+$) cells and LT-HSCs ($CD48^-CD150^+Flt3^-$ LSK) 8 weeks after LT-HSC competitive transplantation. (E, F) The percentage of GFP-positive cells in donor-derived PB and LSK ($Lin^-Sca\text{-}1^+c\text{-}Kit^+$) cells after transplantation with shCDK8 virus infected WT LT-HSCs ($CD48^-CD150^+Flt3^-$ LSK) is shown (n = 4 per group). (G) The knockdown efficiency of shCDK8-1 and shCDK8-2 in virus-infected 3T3 cells. All results are presented as the means ± SD. *p<0.05; **p<0.01; ***p<0.001; Notes: Eight- to twelve-week-old WT and *TRIM31*$^{-/-}$ mice were used in the experiment.

Figure S9. Knockdown of Cyclin D1 rescues the phenotype of *TRIM31*$^{-/-}$ stem cells.

(A, B) The percentage of GFP-positive cells in donor-derived PB and LSK ($Lin^-Sca\text{-}1^+c\text{-}Kit^+$) cells after transplantation with shCyclin D1 virus infected

TRIM31$^{-/-}$ LT-HSCs (CD48^{-}CD150^{+}Flt3^{-} LSK) is shown (n = 4 per group). (C, D) The percentage of GFP-positive cells in donor-derived PB and LSK (Lin^{-}Sca-1^{+}c-Kit^{+}) cells after transplantation with shCyclin D1 virus infected WT LT-HSCs (CD48^{-}CD150^{+}Flt3^{-} LSK) is shown (n = 4 per group). (E) The knockdown efficiency of shCyclinD1-1 and shCyclin D1-2 via real-time PCR. (F) The knockdown efficiency of shCyclin D1 and shCyclin D-2 in virus-infected 3T3 cells. (G) The percentage of G_0 (Ki67 negative) cells from mice 12 weeks after knockdown of Cyclin D1 (n = 4-5 per group). All results are presented as the means ± SD. *p<0.05; **p<0.01; ***p<0.001; NS=not significant. Notes: Eight- to twelve-week-old WT and *TRIM31*$^{-/-}$ mice were used in the experiments.

Figure S10. Overexpression of TRIM31 rescues the phenotype of *TRIM31*$^{-/-}$ stem cells.

(A, B) The percentage of GFP-positive cells among donor-derived PB and LSK cells after transplantation with TRIM31-overexpression virus-infected *TRIM31*$^{-/-}$ LT-HSCs (CD48^{-}CD150^{+}Flt3^{-} LSK) (n = 4 per group). (C) The efficiency of *TRIM31* over-expression via real-time PCR. (D) Representative pictures and of colonies of TRIM31-overexpression virus-infected MLL-AF9 cells after 7 days in culture. Colony number of TRIM31-overexpression (TRIM31-OE) virus-infected MLL-AF9 cells after 7 days in culture (n=3). All results are presented as the means ± SD. *p<0.05; **p<0.01; ***p<0.001; NS=not significant. Notes: Eight- to twelve-week-old WT and *TRIM31*$^{-/-}$ mice were used in the experiments.

Figure S11. Knockdown of PBX1 rescues the phenotype of *TRIM31*$^{-/-}$ stem cells.

(A) The relative mRNA expression of PBX1 and Cyclin D1 in control and PBX1 knockdown or overexpression (PBX1-OE) 3T3NIH cells. The relative expression was normalized to β-actin expression for statistical analysis (n = 3 per group). (B, C) The

percentage of GFP-positive cells in donor-derived PB and LSK ($Lin^-Sca\text{-}1^+c\text{-}Kit^+$) cells after transplantation with shPBX1 virus infected *TRIM31*$^{-/-}$ LT-HSCs ($CD48^-CD150^+Flt3^-$ LSK) is shown (n = 4 per group). (D, E) The percentage of GFP-positive cells in donor-derived PB and LSK ($Lin^-Sca\text{-}1^+c\text{-}Kit^+$) cells after transplantation with shPBX1 virus infected WT LT-HSCs ($CD48^-CD150^+Flt3^-$ LSK) is shown (n = 4 per group). (F) The knockdown efficiency of shPBX1-1 and shPBX1-2 in virus-infected 3T3 cells. (G) The mRNA level of TRIM31, PBX1 and Cyclin D1 in THP1 cells infected with shLuc and shTRIM31 virus was measured via real-time PCR. The relative expression was normalized to β-actin expression for statistical analysis (n = 3 per group). (H) Model of TRIM31-mediated CDK8 function in the hematopoietic system. Ubiquitin-mediated CDK8 degradation is regulated through the E3 ligase TRIM31. CDK8 accumulation is caused by TRIM31 deletion, which further induces upregulation of PBX1 and CyclinD1, ultimately leading to HSC stem cell proliferation and functional decline. All results are presented as the means ± SD. *p<0.05; **p<0.01; ***p<0.001; NS=not significant. Notes: Eight- to twelve-week-old WT and *TRIM31*$^{-/-}$ mice were used in the experiments.

Figure S12. The expressional correlation of CDK8, PBX1 and Cyclin D1.

(A,B) Scatter plot showing expression of the PBX1(A) and Cyclin D1(B) in patients with high (n=44) versus low CDK8 (n=39) expression in AML patients from TCGA dataset. (C) Scatter plot showing expression of the Cyclin D1 in patients with high (n=44) versus low PBX1 (n=48) expression in AML patients from TCGA dataset.

Table S1. Mass spectrometry analysis of TRIM31 interacting proteins.

The selected TRIM31 interacting protein candidates after mass spectrometry analysis are summarized. Notes: Eight- to twelve-week-old WT and *TRIM31*$^{-/-}$ mice were used in the experiments.

Table S2. Primers for qPCR analysis of mRNA transcription.

Table S3. shRNA sequences for genetic knockdown.

Table S4. Primers for detection of the PBX1 promoter region DNA sequence.

Table S5. MS full list of TRIM31 interaction proteins.

Figure S1. *TRIM31* deletion impairs maintenance of progenitors.

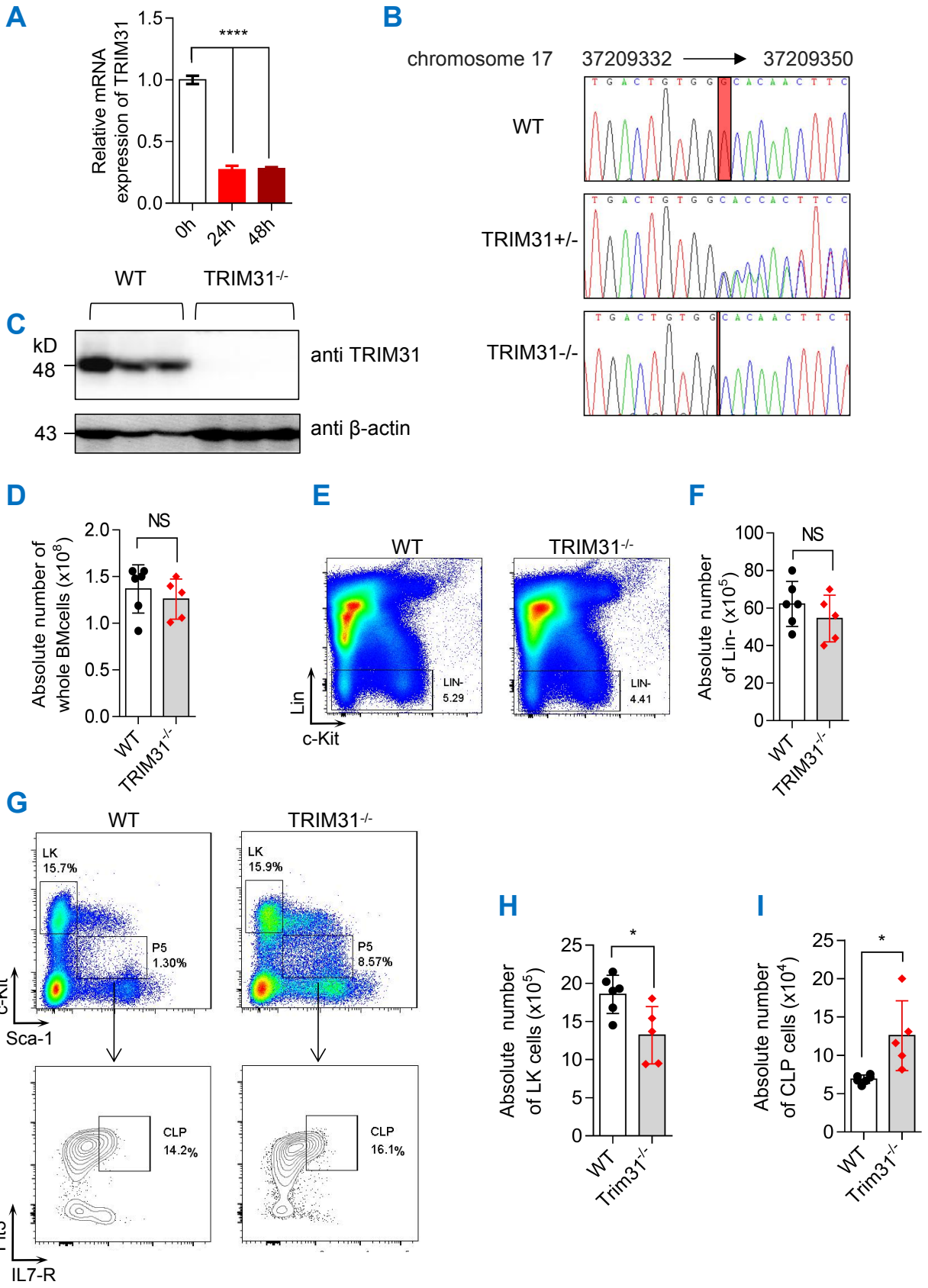

Continuted Figure S1. *TRIM31* deletion impairs maintenance of progenitors.

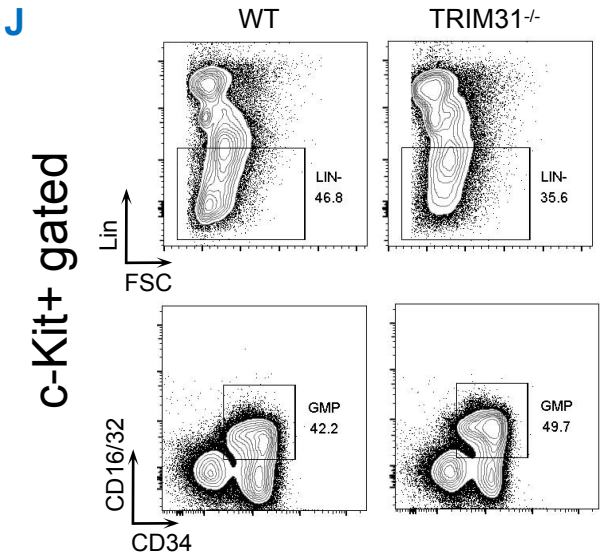

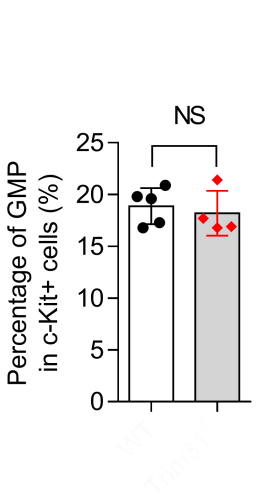

Figure S2. B cells and erythrocytes were affected in *TRIM31*$^{-/-}$ bone marrow.

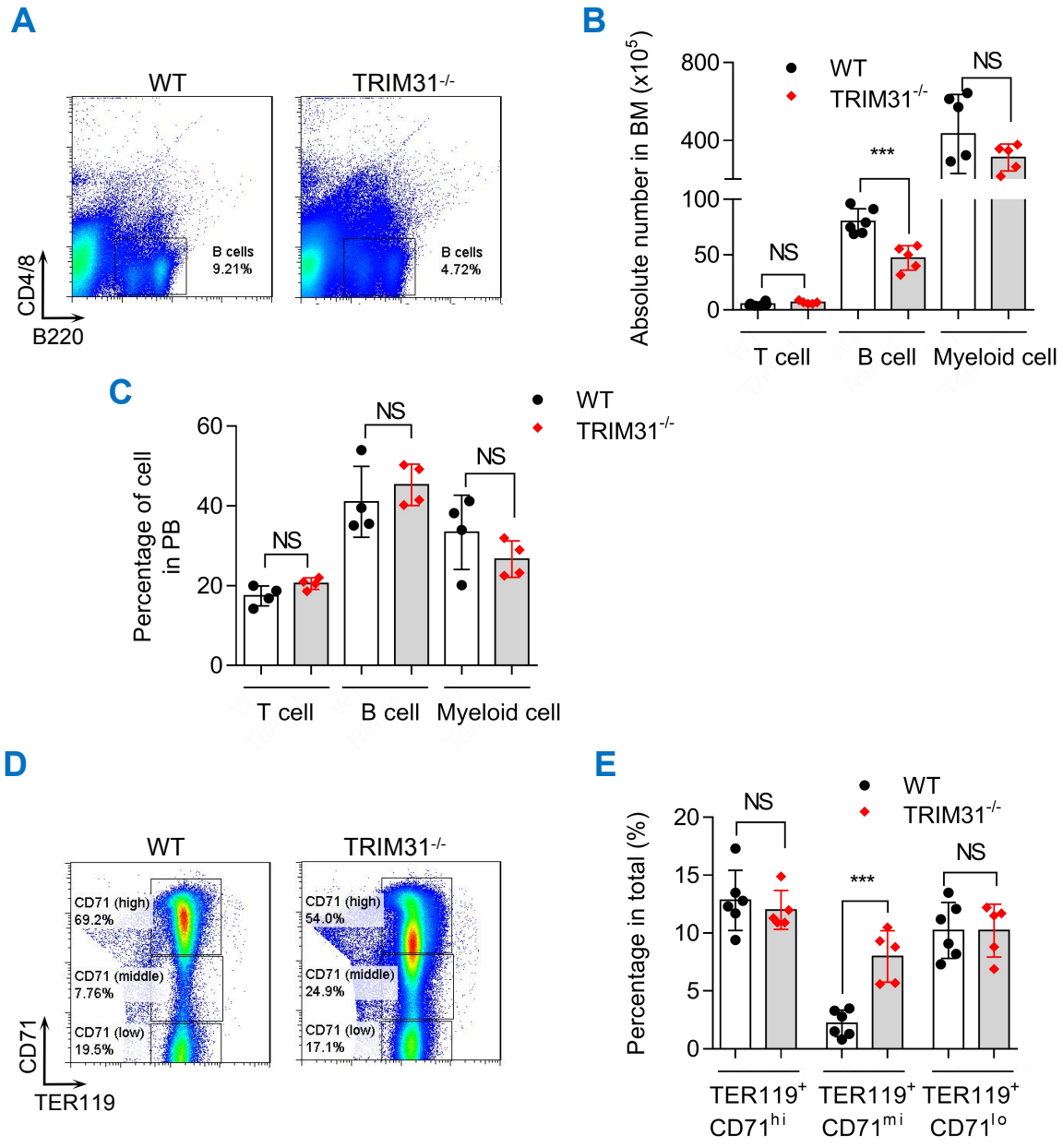

Figure S3. *TRIM31* deficiency causes mouse spleen abnormalities.

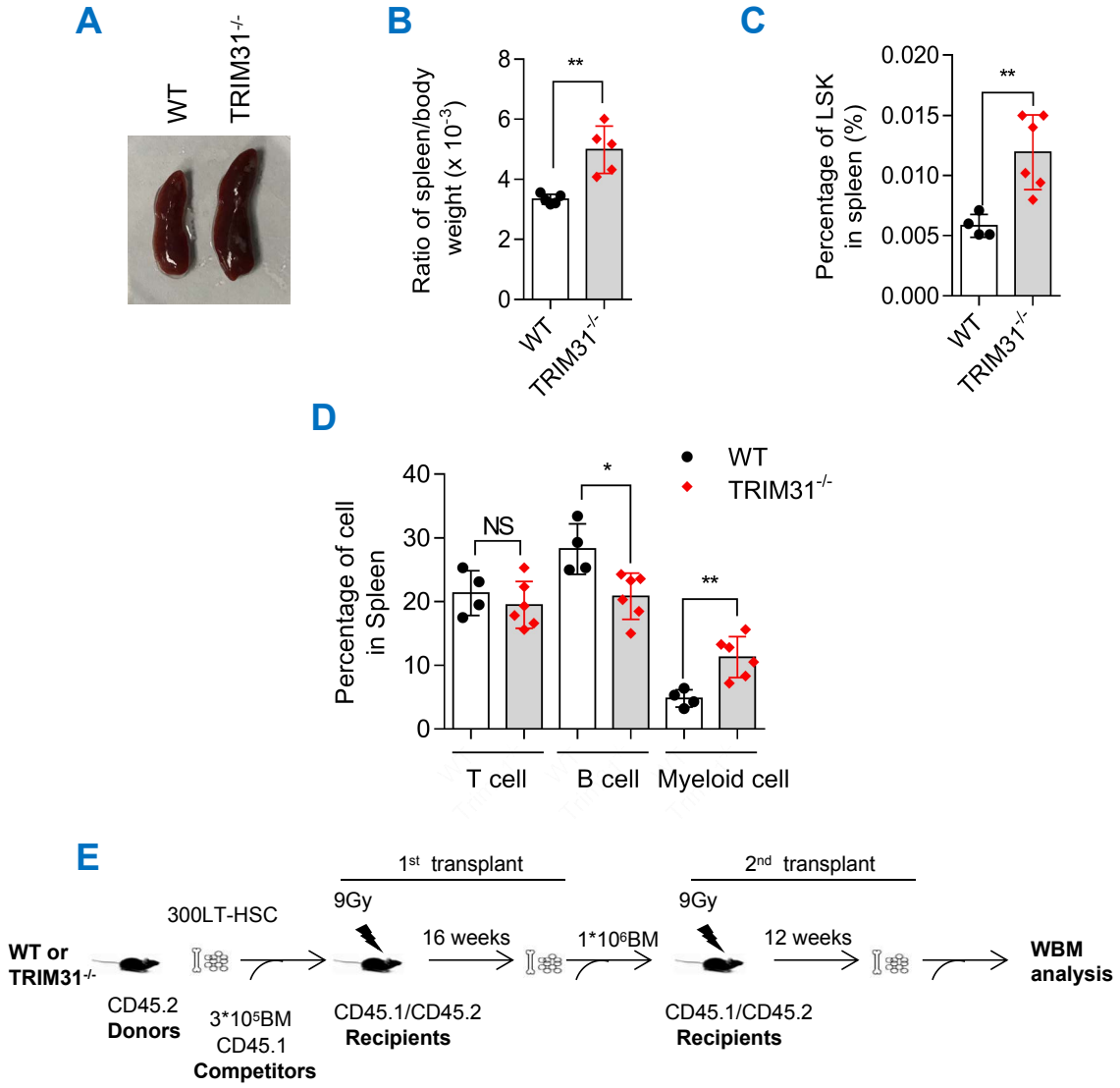

Figure S4. *TRIM31* deletion impairs the self-renewal capacity of LSK cells.

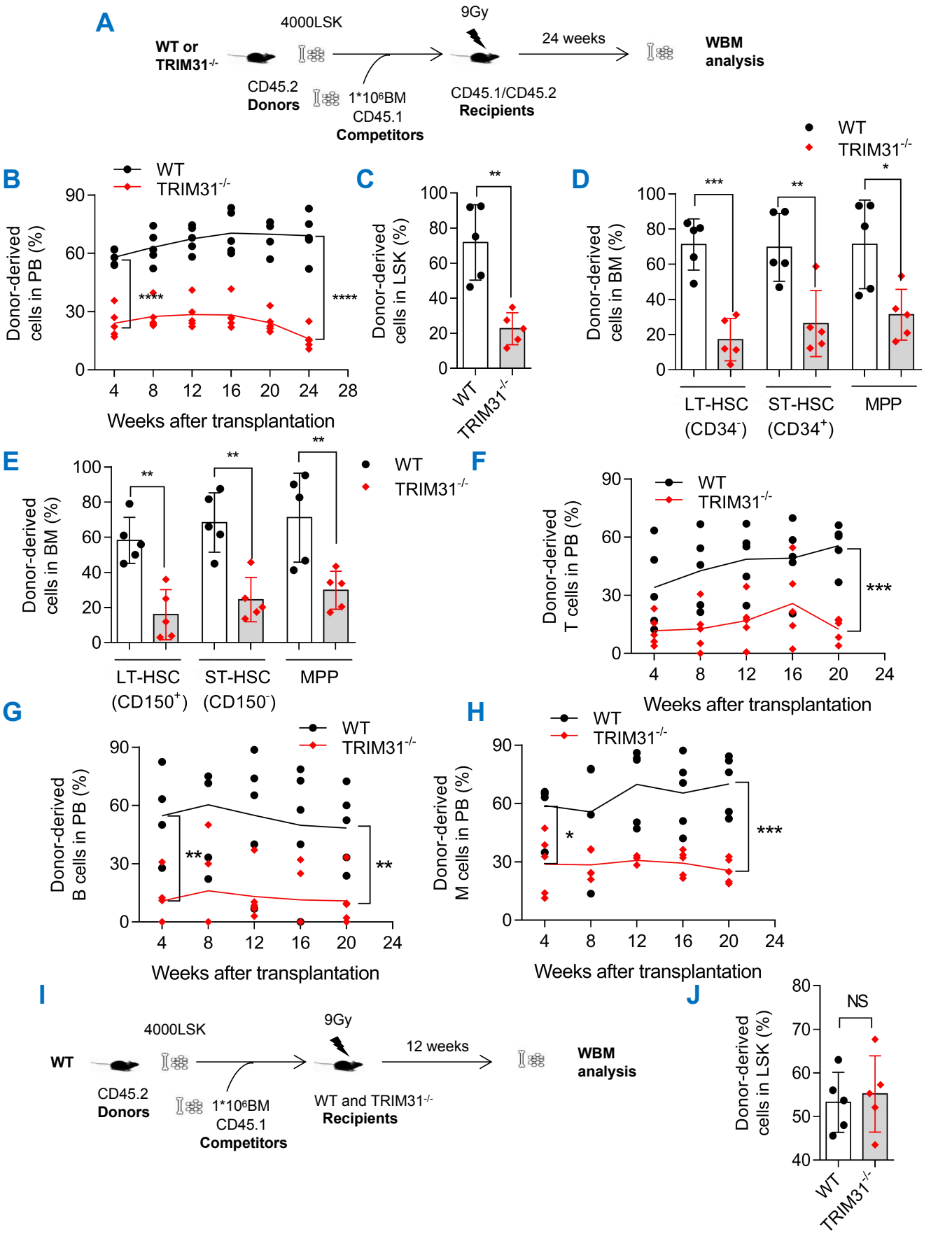

Figure S5. *TRIM31* deletion leads to enhanced HSC proliferation.

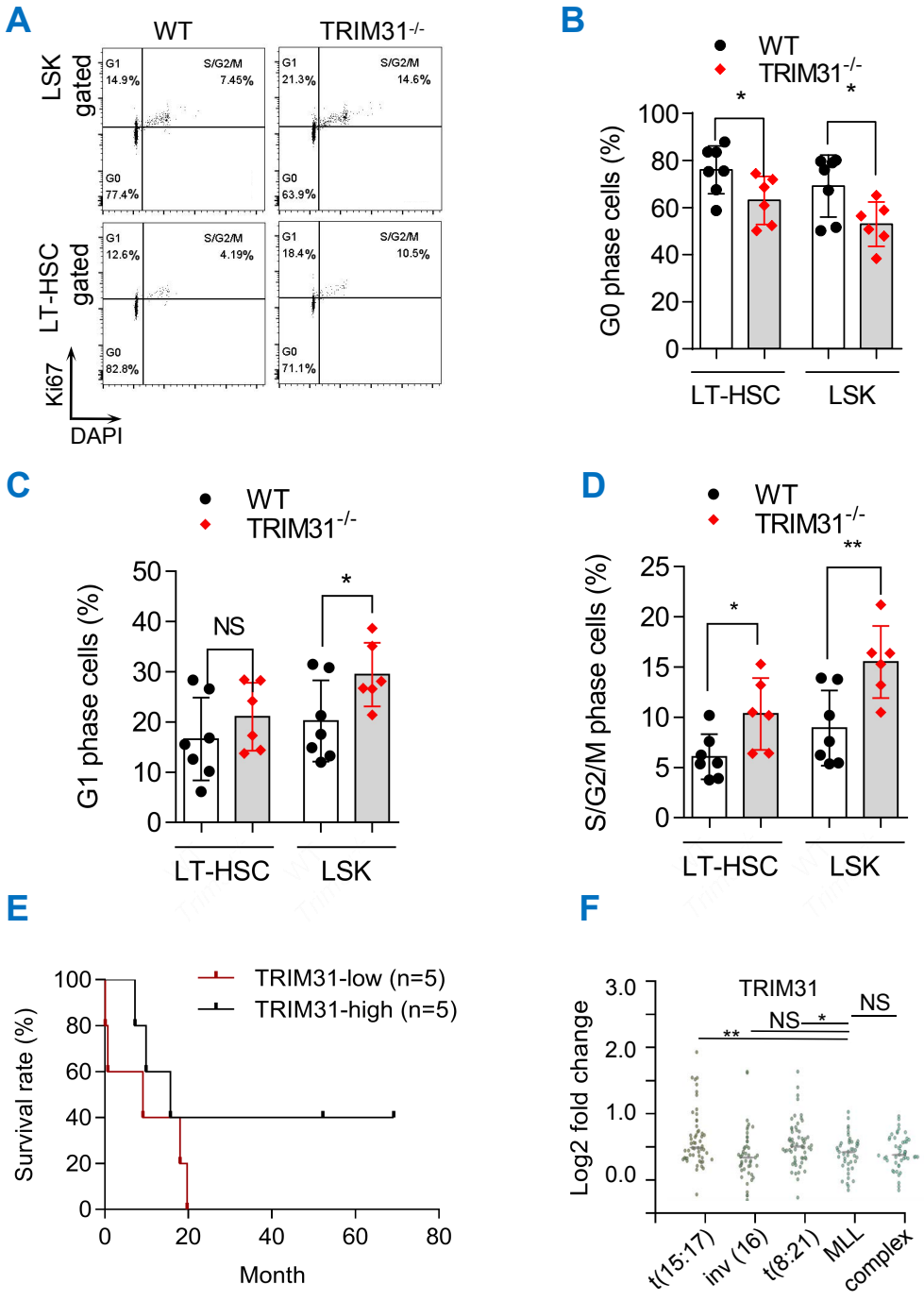

Figure S6. *TRIM31* deficiency accelerated leukemia initiation.

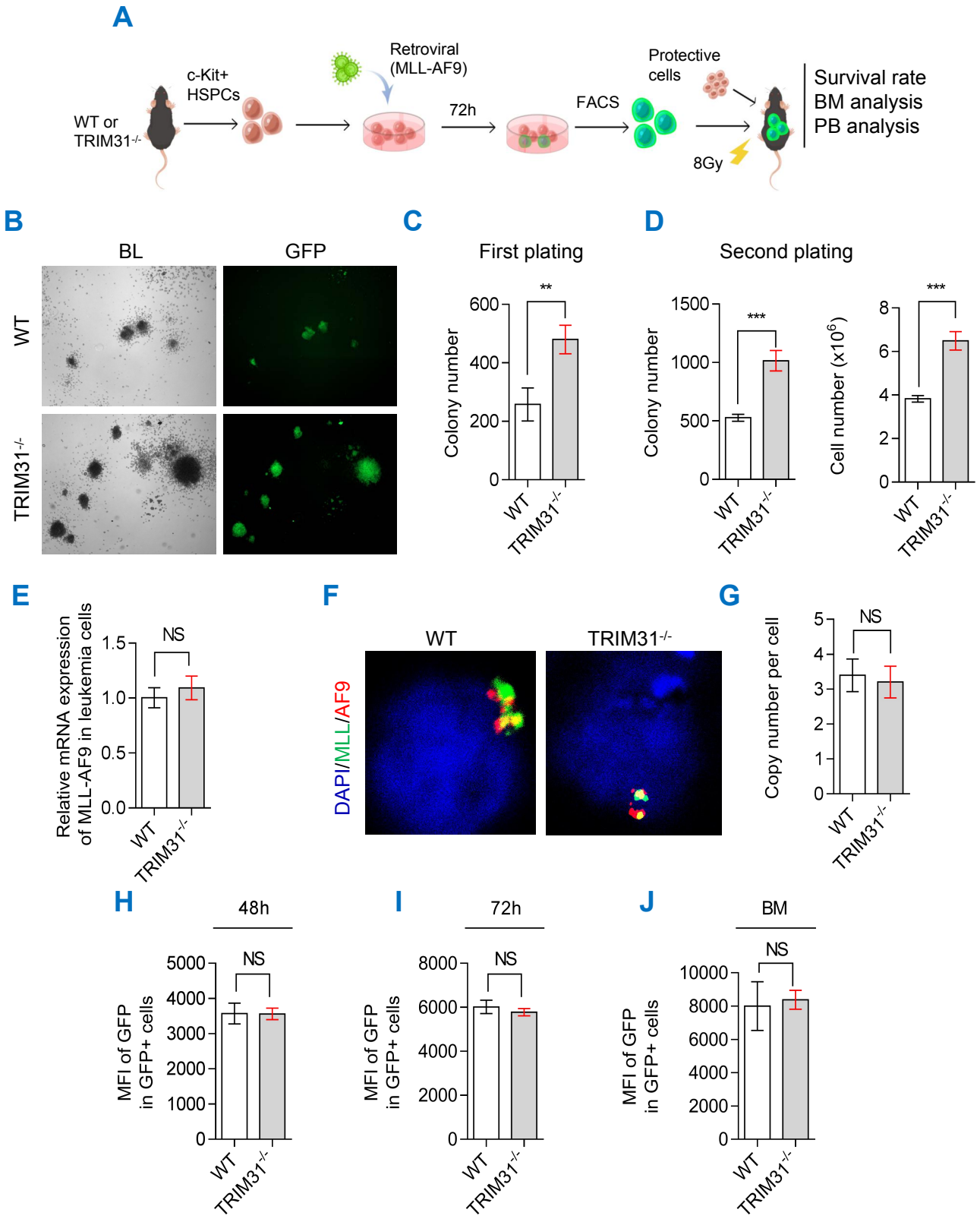

Figure S7. CDK8 associates with Cyclin D1 in hematopoietic cells.

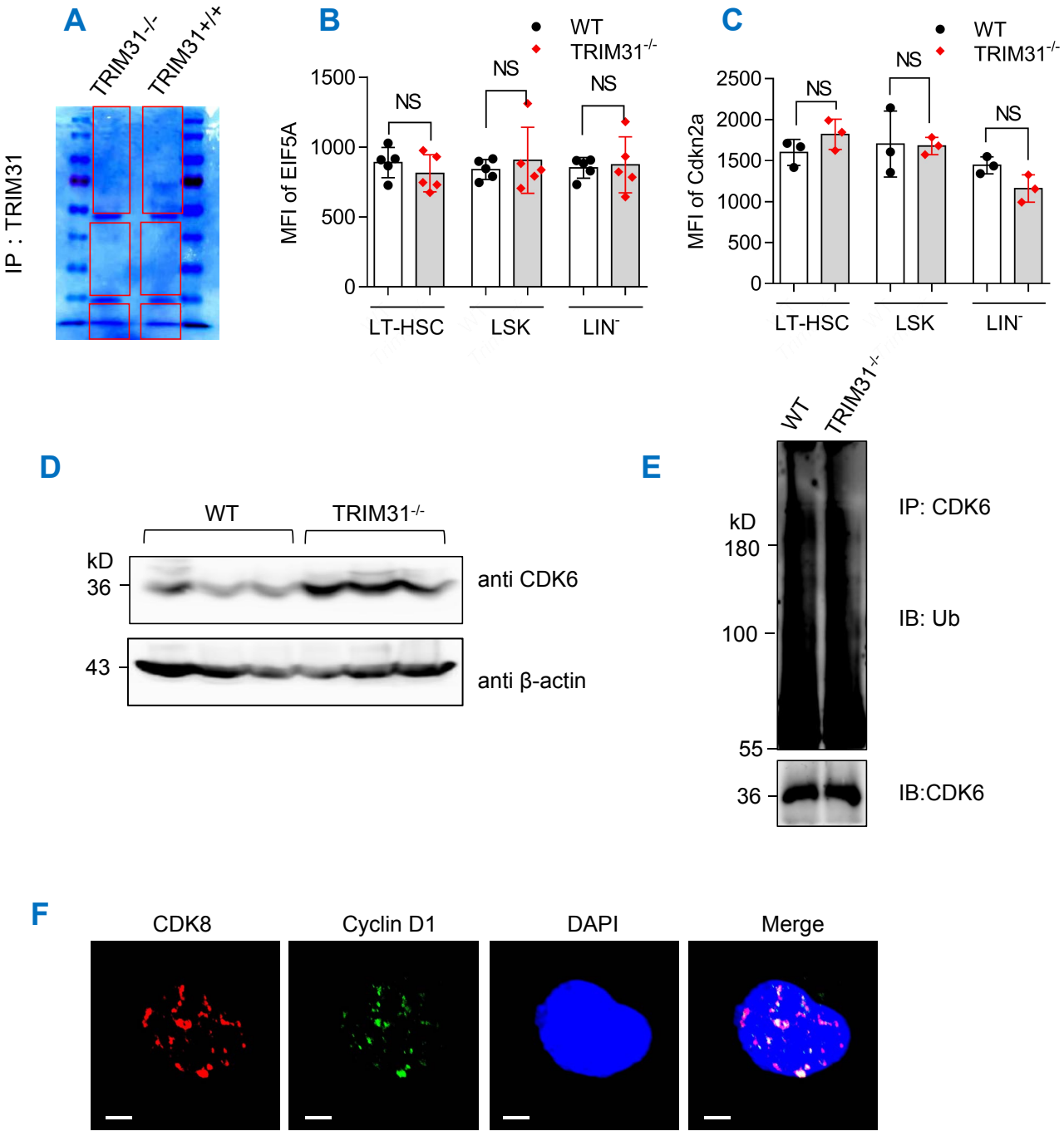

Figure S8. Inhibition and knockdown of CDK8 rescues *TRIM31*$^{-/-}$ HSC function

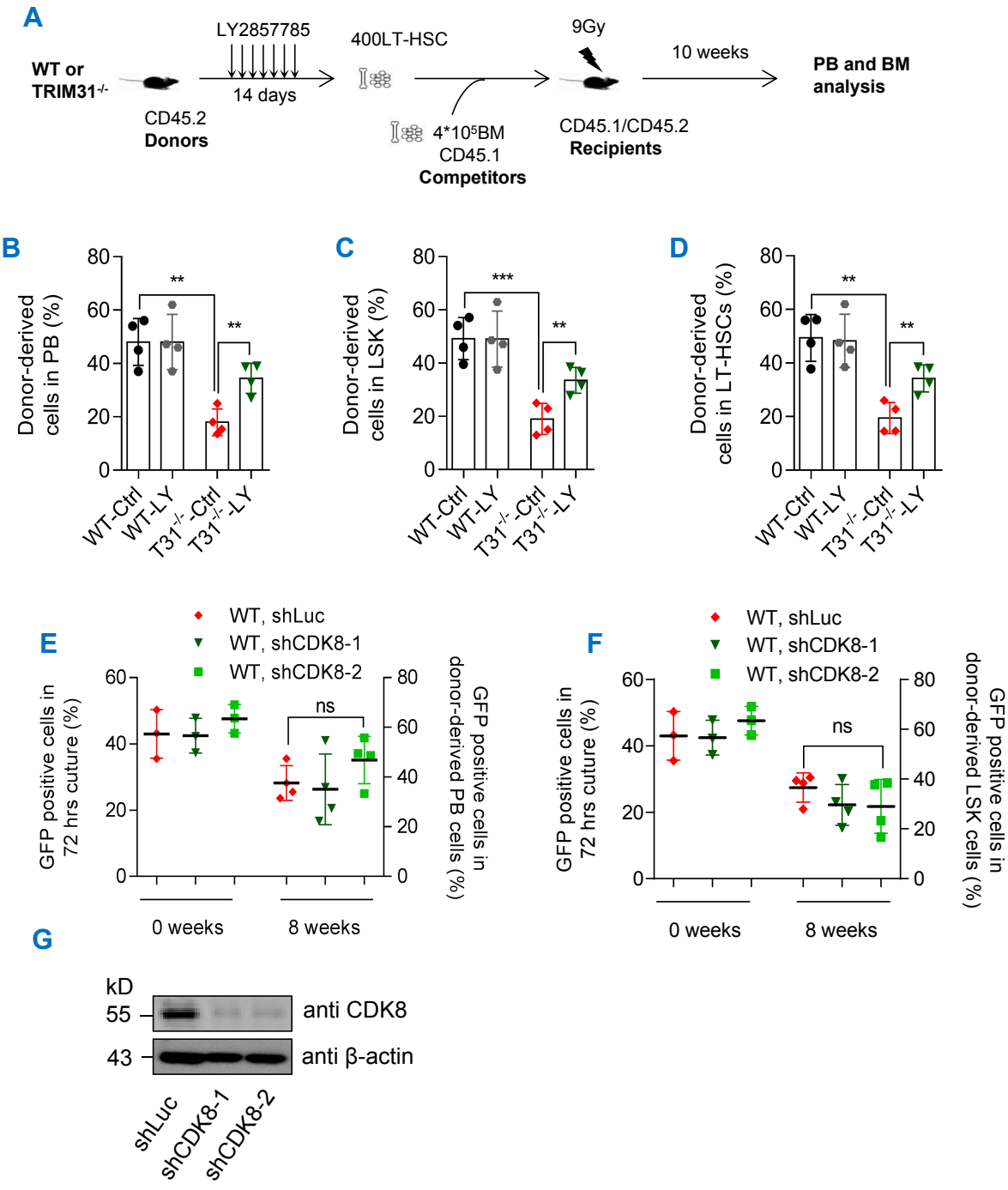

Figure S9. Knockdown of Cyclin D1 rescues the phenotype of *TRIM31*$^{-/-}$ stem cells.

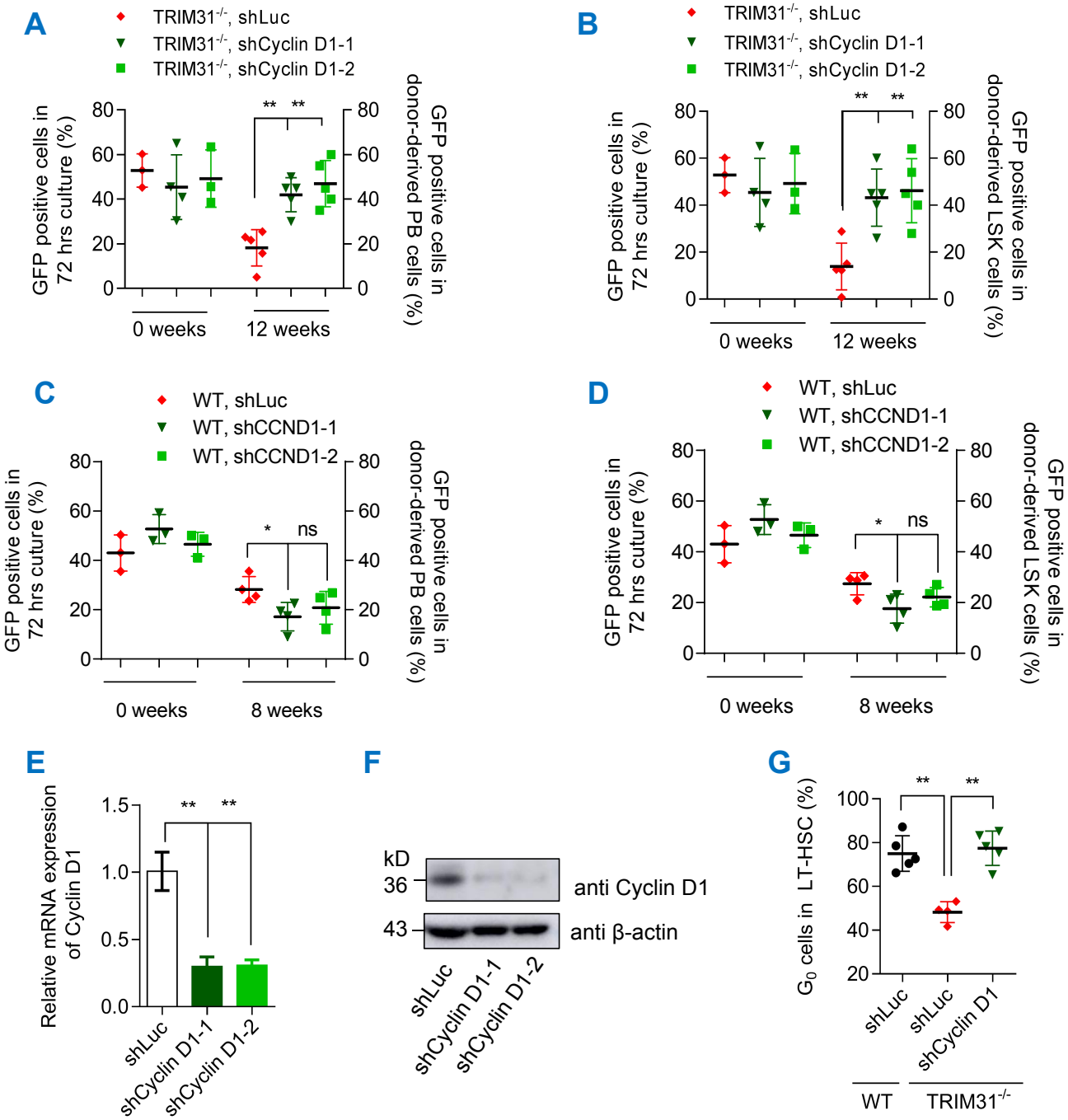

Figure S10. Overexpression of TRIM31 rescues the phenotype of *TRIM31*$^{-/-}$ stem cells.

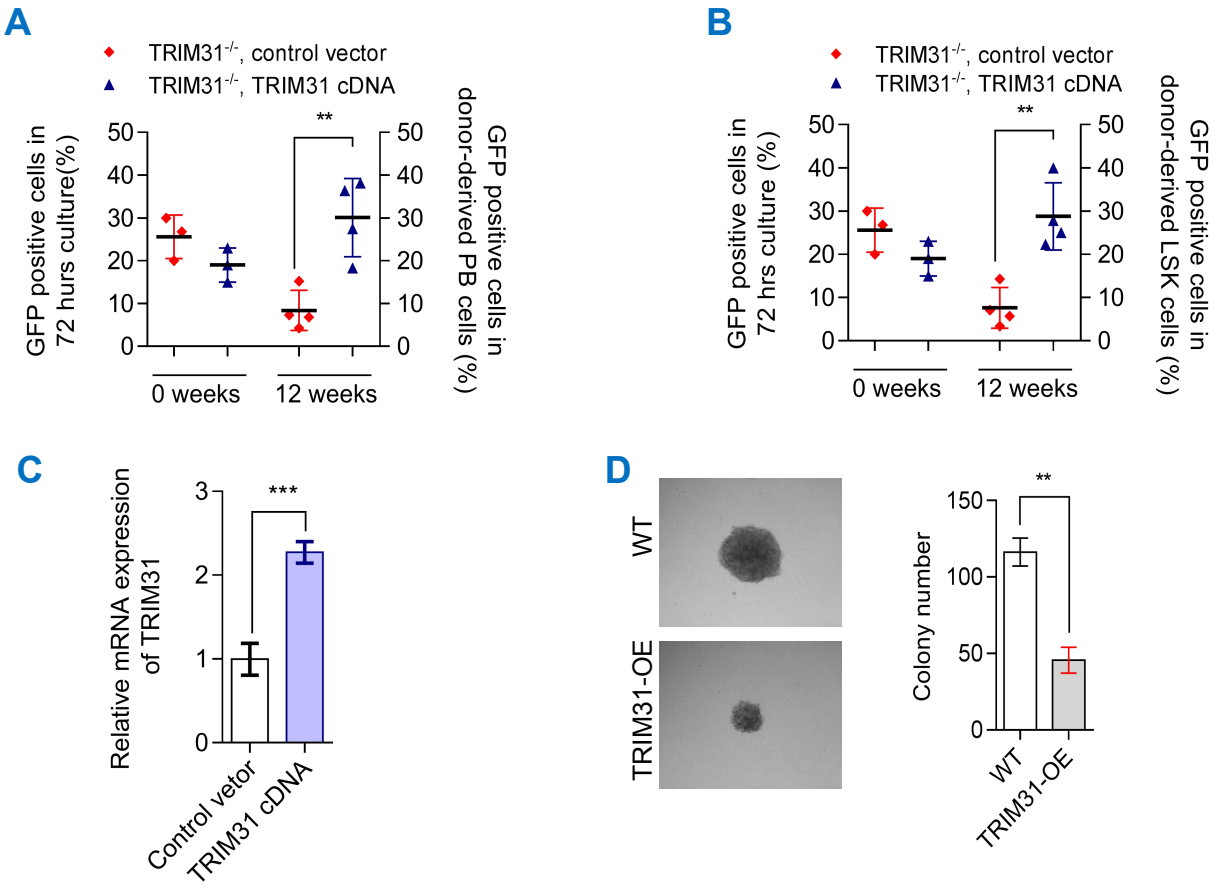

Figure S11. Knockdown of PBX1 rescues the phenotype of *TRIM31*$^{-/-}$ stem cells.

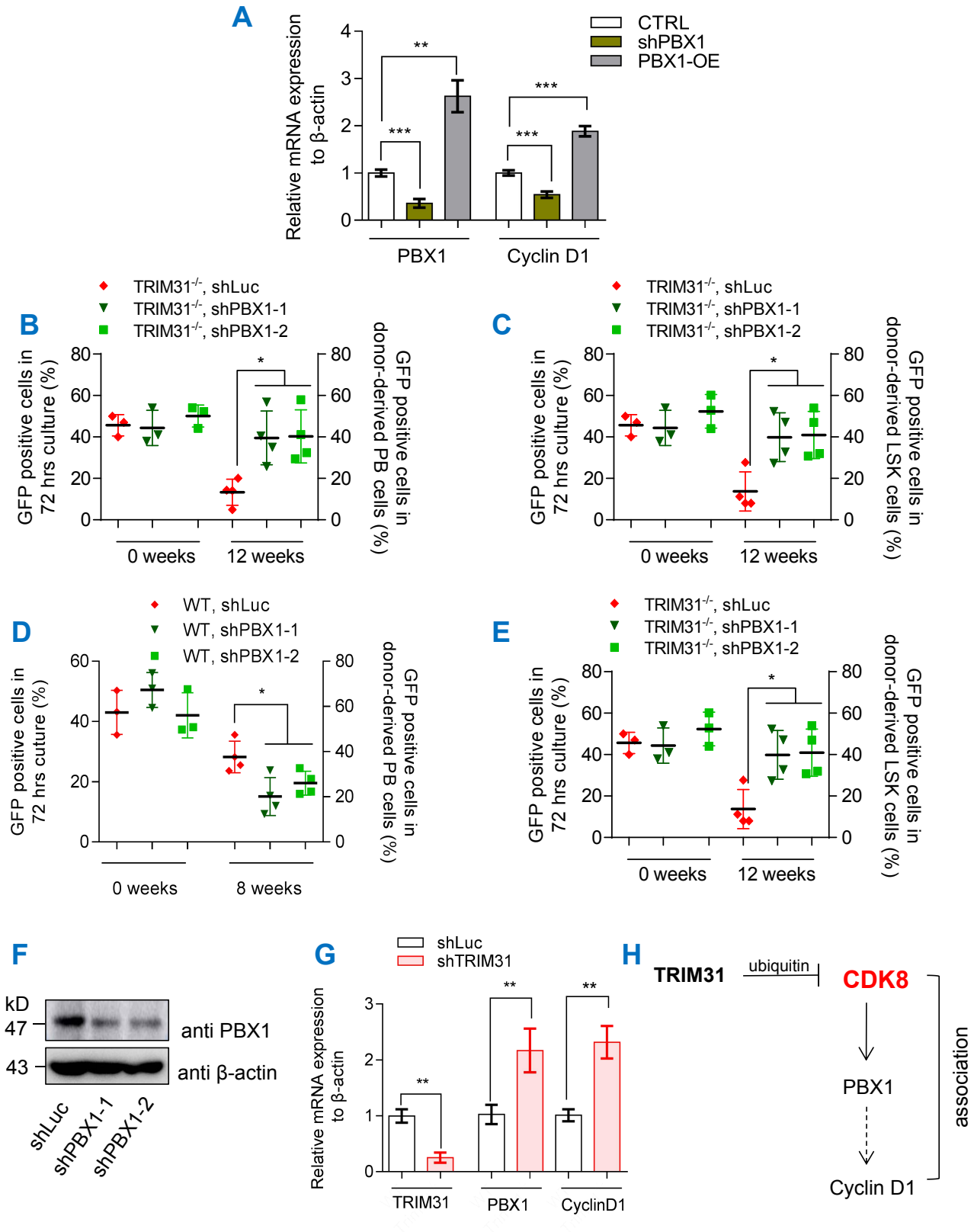

Figure S12. The expressional correlation of CDK8, PBX1 and Cyclin D1.

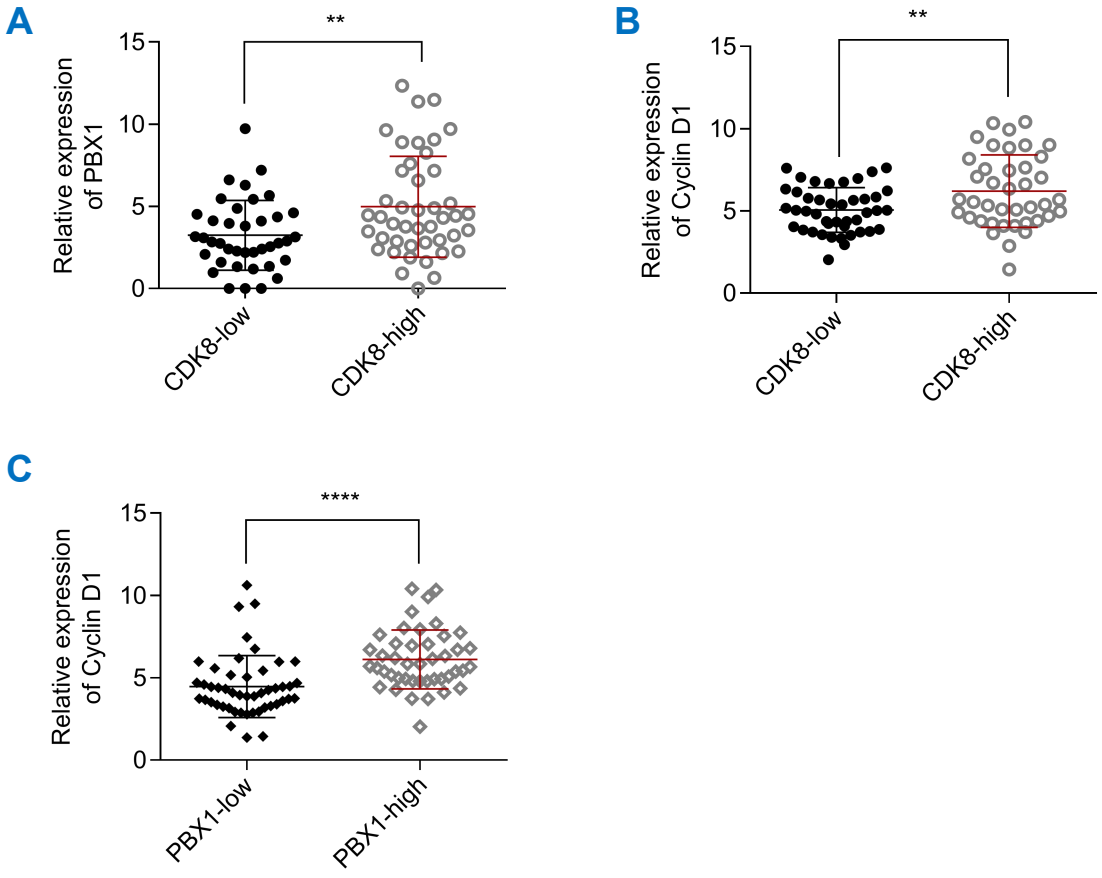

Table S1. Mass spectrometry analysis of TRIM31 interaction proteins.

Protein Name	Pep Count	Unique PepCount	Cover Percent	MW (KD)	PI	Score
Protein kinase C eta type,GN=Prkch	1	1	0.88%	77.9	7.76	22.45
Cyclin-dependent kinase inhibitor 2A,GN=Cdkn2a	1	1	3.57%	17.9	6.04	23.26
Eukaryotic translation initiation factor 5A,GN=EIF5A	1	1	15.58%	16.8	5.07	83.14
Ras-related protein Rab-15, GN=Rab15	1	1	4.35%	16.1	6.75	21.42
Cyclin-dependent kinase 8, GN=CDK8	1	1	3.26%	45.7	8.95	26.13

Table S2. Primer for qPCR analysis of mRNA transcription.

Primer Name	Primer Sequence	Source	Identifer
CDK8-F	GAGAGTTGTCCCTCCTACCACT	Genecards	N/A
CDK8-R	GAGGTAGCTGAGTATCCCATGC	Genecards	N/A
PBX1-F	CAACTCAGTGGAGCATTCCGAC	Genecards	N/A
PBX1-R	GGCTTTGCTCTCGAAGGAGGTT	Genecards	N/A
Cyclin D1-F	GCAGAAGGAGATTGTGCCATCC	Genecards	N/A
Cyclin D1-R	AGGAAGCGGTCCAGGTAGTTCA	Genecards	N/A
β-actin-F	GATCTGGCACCACACCTTCT	This paper	N/A
β-actin-R	GGGGTGTTGAAGGTCTCAAA	This paper	N/A

Table S3. shRNA sequence for genetic knockdown.

Name	Sequence	Source	Identifer
CDK8 shRNA-1	CTCGAGCCGGCCCGATTATTTAATTCA CCTTCTCGAGAAGGTGAATTAAATAATC GGGTTTTTGGAATTC	Sigma-Aldrich	N/A
CDK8 shRNA-2	GCGGCCGCCCGGTACCAAAGCAATTG ATATTTGCTCGAGCAAATATCAATTGCT TTGGTATTTTTGGAATTC	Sigma-Aldrich	N/A
PBX1 shRNA	GCGGCCGCCCGGGCCTGCCTTGTTTAAT GTGTTCTCGAGAACACATTAAACAAGGCA GGCTTTTTGAATTC	Sigma-Aldrich	N/A
Cyclin D1 shRNA-1	GCGGCCGCCCGGGCATCTACACTGACAA CTCTACTCGAGTAGAGTTGTCAGTGTAGA TGCTTTTTGAATTC	Sigma-Aldrich	N/A
Cyclin D1 shRNA-2	GCGGCCGCCCGGCTTTCTTTCCAGAGTC ATCAACTCGAGTTGATGACTCTGGAAAGA AAGTTTTTGGAATTC	Sigma-Aldrich	N/A

Table S4. Primer for the detection of PBX1 promotor region DNA sequence.

Primer Name	Primer Sequence	Source	Identifer
PBX1-1-S	CGGAGGAGGAAAGAGCTTGGG	Self design	N/A
PBX1-1-A	CCGGCGCTTAAATCTGTGGC	Self design	N/A
PBX1-2-S	CGGAGGAGGAAAGAGCTTGGG	Self design	N/A
PBX1-2-A	AATCAGAGCCGCCTTTGGGT	Self design	N/A